AMERICAN SOCIETY FOR MICROBIOLOGY | Journal of Virology®

VIRUS-CELL INTERACTIONS

Identification of ARKL1 as a Negative Regulator of Epstein-Barr Virus Reactivation

Umama Z. Siddiqi,[a] Anup S. Vaidya,[a] Xinliu Li,[a] Edyta Marcon,[b] Sai Wah Tsao,[c] Jack Greenblatt,[a,b] Lori Frappier[a]

[a]Department of Molecular Genetics, University of Toronto, Toronto, Ontario, Canada
[b]Donnelly Centre, University of Toronto, Toronto, Ontario, Canada
[c]School of Biomedical Sciences, Li Ka Shing Faculty of Medicine, The University of Hong Kong, Hong Kong, China

ABSTRACT Epstein-Barr virus (EBV) maintains a life-long infection due to the ability to alternate between latent and lytic modes of replication. Lytic reactivation starts with derepression of the Zp promoter controlling BZLF1 gene expression, which binds and is activated by the c-Jun transcriptional activator. Here, we identified the cellular Arkadia-like 1 (ARKL1) protein as a negative regulator of Zp and EBV reactivation. Silencing of ARKL1 in the context of EBV-positive gastric carcinoma (AGS) cells, nasopharyngeal carcinoma (NPC43) cells, and B (M81) cells led to increased lytic protein expression, whereas overexpression inhibited BZLF1 expression. Similar effects of ARKL1 modulation were seen on BZLF1 transcripts as well as on Zp activity in Zp reporter assays, showing that ARKL1 repressed Zp. Proteomic profiling of ARKL1-host interactions identified c-Jun as an ARKL1 interactor, and reporter assays for Jun transcriptional activity showed that ARKL1 inhibited Jun activity. The ARKL1-Jun interaction required ARKL1 sequences that we previously showed mediated binding to the CK2 kinase regulatory subunit CK2β, suggesting that CK2β might mediate the ARKL1-Jun interaction. This model was supported by the findings that silencing of CK2β, but not the CK2α catalytic subunit, abrogated the ARKL1-Jun interaction and phenocopied ARKL1 silencing in promoting EBV reactivation. Additionally, ARKL1 was associated with Zp in reporter assays and this was increased by additional CK2β. Together, the data indicate that ARKL1 is a negative regulator of Zp and EBV reactivation that acts by inhibiting Jun activity through a CK2β-mediated interaction.

IMPORTANCE Epstein-Barr virus (EBV) maintains a life-long infection due to the ability to alternate between latent and lytic modes of replication and is associated with several types of cancer. We have identified a cellular protein (ARKL1) that acts to repress the reactivation of EBV from the latent to the lytic cycle. We show that ARKL1 acts to repress transcription of the EBV lytic switch protein by inhibiting the activity of the cellular transcription factor c-Jun. This not only provides a new mechanism of regulating EBV reactivation but also identifies a novel cellular function of ARKL1 as an inhibitor of Jun-mediated transcription.

KEYWORDS ARKL1, BZLF1 promoter, CK2, EBV reactivation, Jun

Epstein-Barr virus (EBV) is a gammaherpesvirus that infects over 90% of the worldwide human population (1). Primary infection with EBV is often asymptomatic, but it can present as infectious mononucleosis (IM) if delayed until adolescence. Since its discovery as the first human oncogenic virus, EBV has been tightly associated with several types of malignancies, including Burkitt's and Hodgkin's lymphomas and nasopharyngeal and gastric carcinomas (2–5). Transmitted through saliva, the virus establishes life-long infections through infection of B cells and epithelial cells (6).

EBV alternates between latent and lytic modes of infection. During EBV latency, cells become immortalized through the action of a small number of latency proteins (EBNAs

Citation Siddiqi UZ, Vaidya AS, Li X, Marcon E, Tsao SW, Greenblatt J, Frappier L. 2019. Identification of ARKL1 as a negative regulator of Epstein-Barr virus reactivation. J Virol 93:e00989-19. https://doi.org/10.1128/JVI.00989-19.

Editor Richard M. Longnecker, Northwestern University

Address correspondence to Lori Frappier, lori.frappier@utoronto.ca.

Received 13 June 2019
Accepted 17 July 2019
Accepted manuscript posted online 24 July 2019
Published 30 September 2019

and LMPs) as well as viral microRNAs (miRNAs), and the viral genomes are replicated and maintained in circular form at a constant copy number in the absence of virion production (7, 8). Lytic infection involves the ordered expression of ~80 additional EBV proteins, which leads to amplification of the EBV genomes in linear form and virion production. The switch from latency to lytic infection starts with the expression of the immediate early (IE) gene *BZLF1*, encoding a basic leucine zipper (bZIP) transcriptional activator that activates the expression of EBV immediate early and early lytic genes by binding to AP-1 and AP-1-like sequences termed ZREs (BZLF1-responsive elements) (9–14). In latency, EBV lytic promoters, including the BZLF1 promoter (Zp), are densely covered with nucleosomes containing repressive histone marks, and lytic reactivation involves a switch to active chromatin, including increased histone acetylation and H3K4 trimethylation (15–17). Experimentally, BZLF1 expression can be induced by treatment with histone deacetylase inhibitors (e.g., sodium butyrate [NaB]), 12-*O*-tetradecanoylphorbol-13-acetate (TPA), calcium ionophores (18–21), or cross-linking surface immunoglobulins of B cells using anti-immunoglobulin (anti-Ig) (22).

Expression of the BZLF1 gene is tightly regulated at the transcriptional level by several activator and repressor proteins that bind various elements of Zp (9, 12, 23). Both Sp1 and MEF2 family transcription factors bind to the ZI element of Zp to activate the promoter (24–26). A second critical element for Zp activation is ZII. ZII contains an AP-1/CREB binding site that is bound and activated by several cellular factors, including c-Jun (27–29). Zp also contains ZREs within the ZIII element, which are bound by the BZLF1 protein, leading to increased Zp activity once the lytic cycle is initiated (30). In addition, cellular nucleosome assembly protein TAF-Iβ associates with Zp and induces BZLF1 expression in lytic infection by recruiting MLL1 and increasing histone H3K4 dimethylation and H4K8 acetylation (31). X-box-binding protein 1 (Xbp-1) in combination with activated protein kinase D has also been found to contribute to Zp activation (32). In contrast to these Zp activating factors, Zp has been shown to be suppressed by ZEB1 and ZEB2, which bind ZV elements in Zp (33–35). ZIIR has also been identified as a negative regulatory element in Zp. ZIIR inhibits PKC-mediated activation of Zp, thereby contributing to establishment of latent infection (36, 37).

The EBV protein EBNA1 is expressed in all forms of EBV latency in proliferating cells as well as in lytic infection (38). EBNA1 has multiple roles in latency, including the replication and mitotic segregation of latent EBV episomes, transcriptional activation of some EBV latency genes, and anti-apoptotic functions (38, 39). In addition, EBNA1 contributes to lytic infection. In epithelial cells, this involves the disruption of promyelocytic leukemia (PML) nuclear bodies (NBs) through the degradation of PML proteins (40). The EBNA1-mediated degradation of PML proteins involves the recruitment of CK2 kinase, which phosphorylates PML, triggering its ubiquitination and degradation (41, 42). CK2 is a ubiquitously expressed protein kinase, composed of two catalytic (α or α') and two regulatory (β) subunits, that regulates many cellular processes (43). EBNA1 binds CK2 through a pocket in the CK2β subunit containing a KSSR motif (44). To determine whether any cellular protein interacted with CK2 through the same binding pocket as EBNA1, affinity purification coupled to mass spectrometry (AP-MS) experiments were performed comparing wild-type (WT) and KSSR mutants of CK2β. ARKL1 was identified as the most prevalent cellular protein binding to the KSSR pocket (44). ARKL1 is an uncharacterized protein, whose gene is within a pericentric inversion region of chromosome 18 related to schizophrenia and bipolar affective disorder (45). It has homology to the N-terminal region of Arkadia (RNF111), a SUMO-targeted ubiquitin ligase (STUbL) involved in the degradation of SUMO-modified proteins (46–48). ARKL1 contains two out of the three putative SUMO-interacting motifs (SIMs) of Arkadia but lacks the catalytic RING domain required for ubiquitin ligase function (47). It also contains a polyserine region that resembles the region in EBNA1 that binds the KSSR motif in CK2β (44). In addition, ARKL1 was identified as a protein that is highly SUMO modified in response to influenza virus infection (49).

The finding that EBNA1 and ARKL1 would have to compete for the same binding site on CK2 prompted us to investigate the impact of ARKL1 on EBV infection. Here, we

identify a novel role of ARKL1 in the regulation of EBV reactivation through effects on Zp and BZLF1 gene expression. We further show that this regulation involves ARKL1 interactions with c-Jun and CK2β.

RESULTS

ARKL1 suppresses EBV reactivation. We investigated possible roles of ARKL1 in EBV infection by examining effects of silencing ARKL1. Unlike its homologue Arkadia, we found no evidence that ARKL1 affected the transforming growth factor β (TGF-β signaling pathway) (data not shown), which is consistent with previous reports (47). However, ARKL1 silencing using two different ARKL1-specific small interfering RNAs (siRNAs) in gastric carcinoma cells latently infected with EBV (AGS-EBV) led to increased reactivation of EBV to the lytic cycle, as determined by expression of BZLF1 and BMRF1, which are immediate early and early lytic proteins, respectively. This was seen both when reactivation was induced by NaB/TPA treatment (Fig. 1A and B) and for spontaneous reactivation (Fig. 1C and D; for the effect of NaB/TPA treatment on lytic protein induction see Fig. 1E). In the spontaneous reactivation experiment, samples were also analyzed for BZLF1 transcripts by reverse transcriptase quantitative PCR (RT-qPCR) (Fig. 1F). The results show that ARKL1 silencing increases the level of BZLF1 transcripts, suggesting that ARKL1 suppresses BZLF1 expression and subsequent EBV reactivation.

We then investigated whether ARKL1 overexpression had the opposite effect as ARKL1 silencing and suppressed EBV reactivation. To this end, AGS-EBV cells were transfected with FLAG-ARKL1 and then treated with NaB/TPA to induce reactivation. Cells were stained for FLAG to identify transfected cells and for the BZLF1 immediate early protein as a marker for EBV reactivation. The percentage of FLAG-positive and FLAG-negative cells expressing BZLF1 were then determined. Since we have previously observed that transient overexpression of any protein can increase EBV reactivation (50) (possibly due to a stress response), we also included a control of an overexpressed FLAG-tagged protein that is unrelated to EBV infection (FLAG-DDX24). Overexpression of FLAG-ARKL1 was found to significantly decrease the percentage of reactivated cells, compared with both untransfected and FLAG-DDX24-expressing cells (Fig. 2A). Similar experiments were also performed in the absence of NaB/TPA induction to examine the effects of ARKL1 on spontaneous reactivation (Fig. 2B). Again, FLAG-ARKL1 significantly decreased reactivation relative to FLAG-DDX24, which was used as the negative control. A comparison of FLAG-ARKL1 to additional FLAG-tagged proteins (FBXO38 and EBV BKRF4) also confirmed that FLAG-ARKL1 suppressed spontaneous reactivation (Fig. 2C). In addition, the effect of FLAG-ARKL1 overexpression on BZLF1 transcripts was quantified by RT-qPCR, confirming that ARKL1 decreases BZLF1 transcripts (Fig. 2D). Together, the results indicate that ARKL1 can suppress EBV reactivation in AGS-EBV cells by decreasing BZLF1 transcription.

To determine whether ARKL1 also regulated EBV reactivation in other cell backgrounds, we examined the effect of ARKL1 silencing in NPC43 nasopharyngeal carcinoma and M81 B cells. The NPC43 cell line was recently established from biopsy specimens of recurrent nasopharyngeal carcinoma (NPC) and stably retains its original EBV genome (51). A proportion (~10%) of these cells spontaneously enter the lytic cycle, unless the cells are maintained in ROCK inhibitor (51), making them an excellent system for examining spontaneous EBV reactivation. Due to low transient transfection efficiency of these cells, we silenced ARKL1 by transduction with lentiviruses expressing three different short hairpin RNAs (shRNAs) targeting ARKL1 and then examined effects on BZLF1 expression. All three ARKL1-targeted shRNAs decreased the levels of ARKL1 and led to an increase in BZLF1 compared with negative-control shRNAs (Fig. 3A and B). These results are consistent with those in AGS-EBV cells.

We also examined effects of ARKL1 silencing in B cells transformed with M81 EBV (52). Unlike most EBV-transformed B cells, a significant proportion of these cells undergo spontaneous reactivation. These cells were transduced with the lentiviruses expressing three different ARKL1-targeted shRNAs (or negative-control

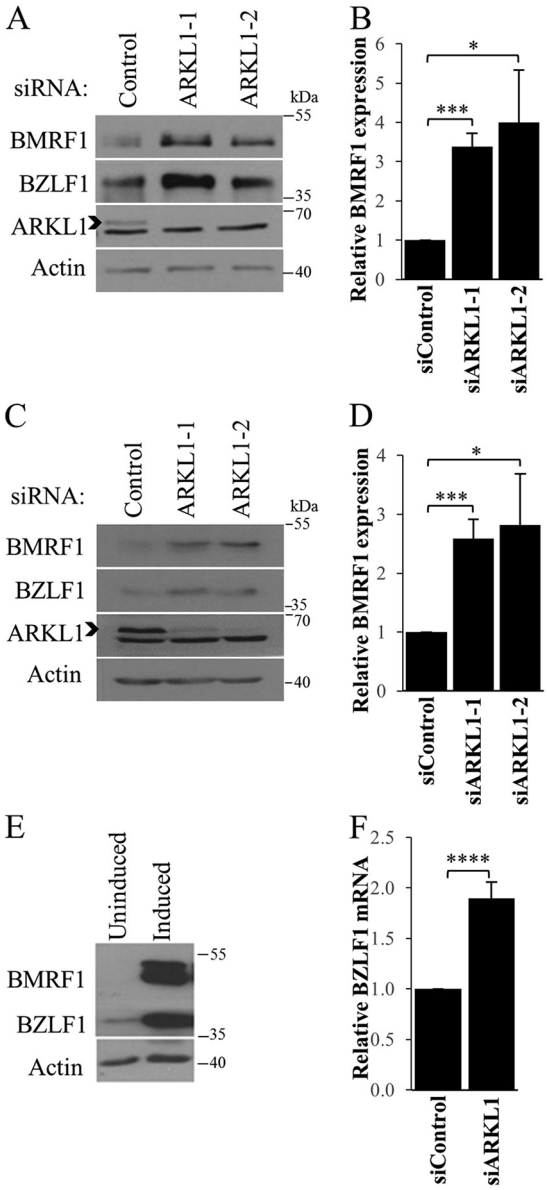

FIG 1 ARKL1 silencing promotes EBV reactivation in AGS-EBV cells. (A) AGS-EBV cells were treated with siRNAs against ARKL1 or negative-control siRNA, and then reactivation was induced with NaB/TPA for 24 hours. A total of 30 μg of lysates was compared by Western blotting using antibodies against ARKL1, BMRF1, BZLF1, and actin. (B) Quantification of BMRF1 bands from three experiments performed as in (A). (C) AGS-EBV cells were treated with siRNAs against ARKL1 or negative-control siRNA, and then 100 μg of lysates were compared by Western blotting as in (A). (D) Quantification of BZLF1 bands from three experiments performed as in (C). (E) Western blot comparing 30 μg of lysates from induced and uninduced samples from (A and C). Exposure time used was longer than in panel A. (F) AGS-EBV cells were transfected with siRNA targeting ARKL1 or negative-control siRNA as in (C), followed by quantification of BZLF1 transcripts by RT-qPCR. BZLF1 mRNA levels were normalized to actin mRNA and are shown relative to negative-control siRNA. Average values from three separate experiments with standard deviations are shown. *, $0.01 < P < 0.05$; ***, $P < 0.001$; ****, $P < 0.0001$.

shRNA). All three shARKL1 lentiviruses resulted in stable cell lines with decreased levels of ARKL1. A comparison of the BZLF1 levels showed that ARKL1 depletion resulted in an obvious increase in BZLF1 (Fig. 3C and D), consistent with increased reactivation. Quantification of BZLF1 transcripts in these cells confirmed that ARKL1 depletion resulted in increased transcription of BZLF1 (Fig. 3E). Together, our results indicate that ARKL1 can suppress EBV reactivation in multiple cell backgrounds relevant for EBV infection by suppressing BZLF1 transcription.

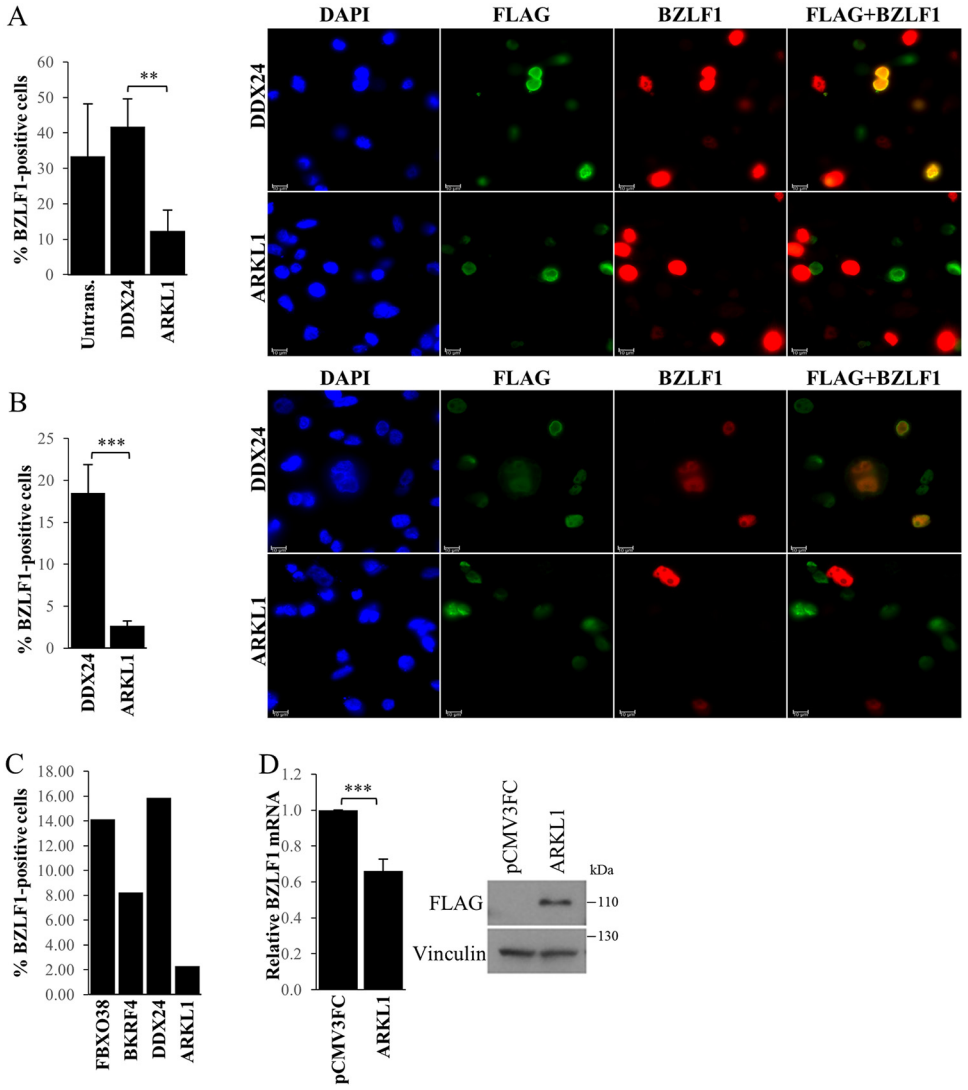

FIG 2 ARKL1 overexpression inhibits EBV reactivation in AGS-EBV cells. (A) AGS-EBV cells were transfected with plasmids expressing FLAG-ARKL1 or FLAG-DDX24 and then treated with NaB/TPA. Twenty-four hours later, cells were fixed and stained with antibodies against FLAG and BZLF1, and the percentage of FLAG-positive cells expressing BZLF1 was determined. Untransfected FLAG-negative cells expressing BZLF1 are also shown (Untrans.). At least 100 transfected cells were counted for each experiment. Average values from three separate experiments with standard deviations are shown. Representative images of cells stained with DAPI, FLAG, and BZLF1 are also displayed. (B) AGS-EBV cells were transfected and processed as in (A) except that cells were not treated with NaB/TPA. (C) AGS-EBV cells were transfected with plasmids expressing FLAG-FBXO38, FLAG-BKRF4, FLAG-DDX24, or FLAG-ARKL1, and the percentage of BZLF1-positive cells was compared. (D) AGS-EBV cells were transfected with FLAG-ARKL1 or empty FLAG (pCMV3FC) expression plasmids as in (B) followed by quantification of BZLF1 transcripts by RT-qPCR. BZLF1 mRNA levels were normalized to actin mRNA and shown relative to empty plasmid control. The averages from three experiments along with their standard deviations are shown. **, $0.001 < P < 0.01$; ***, $P < 0.001$. A Western blot is also shown to confirm expression of FLAG-ARKL1 (relative to vinculin loading control).

ARKL1 suppresses the BZLF1 promoter. Since ARKL1 affects expression of the BZLF1 lytic switch protein, we asked whether ARKL1 acts on the BZLF1 promoter (Zp). The activity of Zp can be assessed using a luciferase reporter construct in which expression of the firefly luciferase gene is under the control of Zp (53). This reporter plasmid was cotransfected with FLAG-ARKL1 expression plasmid or empty FLAG plasmid along with a renilla reporter plasmid as a transfection control. Luciferase activity was then quantified and normalized to renilla. ARKL1 overexpression consistently decreased luciferase expression, indicating suppression of Zp (Fig. 4A). We then silenced ARKL1 with siRNA (ARKL1-1 from Fig. 1) and repeated the Zp-luciferase reporter

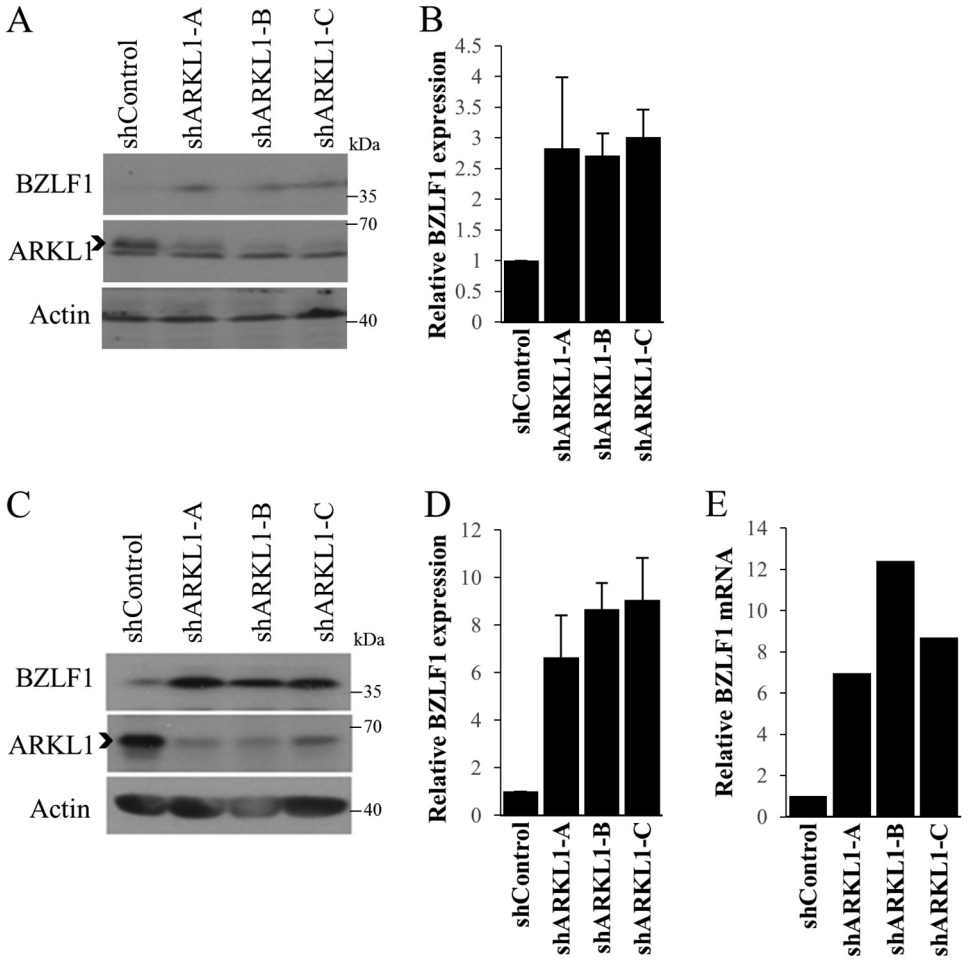

FIG 3 ARKL1 silencing promotes EBV reactivation in NPC43 and M81 B cells. (A) NPC43 cells were transduced with lentivirus expressing three different shRNAs (A, B, and C) targeting ARKL1 or negative-control shRNA (shControl). Equal amounts of lysates were compared by Western blotting using antibodies against ARKL1, BZLF1, and actin. (B) Quantification of BZLF1 bands from two experiments performed as in (A), showing averages and standard deviations. (C) M81 B cells were transduced with lentivirus expressing three different ARKL1-specific shRNAs or negative-control shRNA, and equal amounts of lysates were compared by Western blotting. (D) Quantification of BZLF1 bands from two experiments performed as in (C), showing averages and standard deviations. (E) M81 B cells transduced with ARKL1 shRNAs or negative-control shRNA as in (C) were harvested for RT-qPCR analysis of BZLF1 mRNA transcripts. Levels of the BZLF1 transcripts normalized to actin are shown relative to the control shRNA.

assay. Compared with the negative-control siRNA treatment, ARKL1 silencing significantly increased luciferase expression, indicating increased Zp activity (Fig. 4B). Therefore, ARKL1 represses the BZLF1 promoter to regulate BZLF1 expression.

ARKL1 interacts with and suppresses the activity of c-Jun. To gain insight into the mechanism by which ARKL1 might regulate Zp and EBV reactivation, we used affinity purification coupled to mass spectrometry (AP-MS) to identify the protein interactions of ARKL1. To this end, FLAG-ARKL1 was transiently expressed in 293T cells and recovered on anti-FLAG resin under stringent conditions, and eluted proteins were analyzed by liquid chromatography-tandem mass spectrometry (LC-MS/MS). The most prevalent interactors identified with FLAG-ARKL1 in two independent experiments and not found in the FLAG negative-control are shown in Table 1 (indicated by total spectral counts). We also compared the recovery of each protein to the average spectral counts in the Contaminant Repository of Affinity Purification database (http://www.crapome.org/) (54) to rule out nonspecific interactions. CK2 protein subunits were the top interactors of ARKL1, which is consistent with our previous finding that ARKL1 is a prevalent interactor of CK2β (44). Among the ARKL1 interactors was the AP-1 tran-

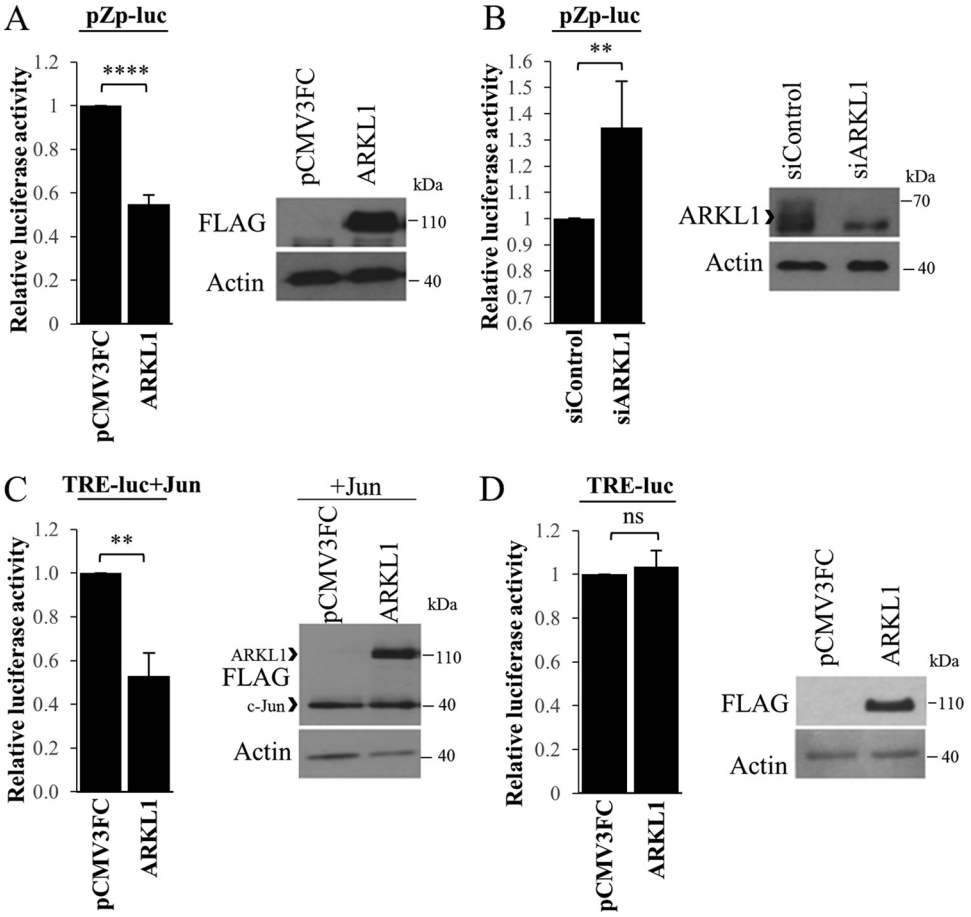

FIG 4 ARKL1 suppresses Zp and Jun activity in reporter assays. (A) AGS cells were cotransfected with pZp-luc (firefly luciferase) and pRL-TK (renilla) reporter plasmids along with FLAG-ARKL1 or empty FLAG (pCMV3FC) expression plasmids. (B) AGS cells were transfected with siRNA targeting ARKL1 or negative-control siRNA, followed by transfection with pZp-luc and pRL-TK reporter plasmids. (C) AGS cells were transfected with plasmids expressing c-Jun and either FLAG-ARKL1 or empty FLAG (pCMV3FC) along with 5XTRE-luciferase and pRL-TK reporter plasmids. (D) AGS cells were transfected with plasmids expressing FLAG-ARKL1 or empty FLAG (pCMV3FC) along with 5XTRE-luciferase and pRL-TK reporter plasmids. In all cases, cells were harvested 48 h post-plasmid transfection, and firefly luciferase and renilla were quantified in a luminometer. Raw luciferase values were over 10,000 units for all experiments. Average luciferase values from multiple experiments (four for A and B and three for C and D) after normalization to renilla are shown, along with the representative Western blots for the expression of the transfected plasmids. ns, no significance; **, $0.001 < P < 0.01$; ****, $P < 0.0001$.

scription factor c-Jun, which was previously identified as an important activator of Zp (14, 18, 20, 23, 26, 55). The interaction of ARKL1 with Jun was then confirmed by immunoprecipitation in AGS cells, where transient expression of FLAG-ARKL1 efficiently recovered endogenous Jun (Fig. 5A).

The interaction of ARKL1 with Jun suggested a mechanism by which ARKL1 might suppress Zp, by binding to and inhibiting the activation function of Jun. Therefore, we tested whether ARKL1 affected Jun activity using a luciferase reporter under the control of Jun binding sites (5xTRE) and normalized to effects on the renilla reporter. When coexpressed with Jun, ARKL1 inhibited the ability of Jun to activate the luciferase reporter (Fig. 4C). As a control, we also measured the effects of ARKL1 overexpression in the absence of Jun overexpression (Fig. 4D). As expected, the ability of ARKL1 to repress the Jun-luciferase reporter was dependent on Jun. These results are consistent with our model that ARKL1 represses Zp by negatively regulating Jun activity.

ARKL1 binds Jun through CK2β. We have previously shown that the interaction of ARKL1 with CK2β involves the polyserine region of ARKL1 (amino acids 202 to 226), such that deletion of this region in ARKL1 (ARKL1ΔS) abrogates CK2β binding (44). In

TABLE 1 Affinity Purification-Mass Spectrometry of ARKL1

Protein ID[a]	Protein identified	Total spectral counts of:[b]				
		FLAG-ARKL1		FLAG-pCMV3FC		CRAPome avg
		Expt 1	Expt 2	Expt 1	Expt 2	
Q96B23	C18orf25 (ARKL1)	510	642	0	0	0
P68400	CK2α	309	208	0	0	2.9
P67870	CK2β	251	104	0	0	1.6
P19784	CK2α'	197	106	0	0	1.5
Q9BVP2	GNL3	21	39	0	0	5.5
Q92598	HSPH1	19	46	0	0	6
P49458	SRP9	16	11	0	0	1.7
P61289	PSME3	15	42	0	0	4.4
Q9BQ67	GRWD1	8	22	0	0	2.7
P37108	SRP14	8	17	0	0	2.6
P05412	Jun	7	9	0	0	1.5
P35659	DEK	5	9	0	0	2.8

[a]ID, identifier.
[b]Total spectral counts for two independent experiments with FLAG-ARKL1 or empty FLAG (negative control) are shown. Average spectral counts reported for each protein in the CRAPome database are also shown for comparison.

the course of verifying the ARKL1-CK2β interaction, we found that endogenous Jun was efficiently immunoprecipitated by FLAG-ARKL1 but was not detected with FLAG-ARKL1ΔS (Fig. 5A). This raised the possibility that ARKL1 might associate with Jun through CK2β (or the CK2 holoenzyme). We tested this possibility in two ways. First, we asked whether Jun could interact with either CK2 subunit. To this end, we expressed FLAG-tagged CK2α or CK2β and performed FLAG immunoprecipitations (IPs) to compare recovery of endogenous Jun (Fig. 5B). Despite lower expression levels and recovery of CK2β compared to CK2α, Jun was clearly recovered with CK2β but not CK2α. Second, we asked whether silencing CK2α or CK2β affected the ability of FLAG-ARKL1 to immunoprecipitate endogenous Jun (Fig. 5C). To this end, CK2α (lanes 5 and 6) or CK2β (lanes 3 and 4) were efficiently silenced in AGS cells with siRNA compared with siControl samples (lanes 1 and 2), followed by transfection of FLAG-ARKL1 or empty FLAG plasmids and FLAG IP. Jun was recovered with FLAG-ARKL1 in both siControl or CK2α-silenced samples (lanes 8 and 12) but not detected in the CK2β-silenced sample (lane 10), indicating that CK2β but not CK2α is needed for the Jun-ARKL1 interaction. Together, the data suggest that the interaction between Jun and ARKL1 is mediated by CK2β.

CK2β suppresses EBV reactivation. If our model is correct that ARKL1 associates with Jun through CK2β and that this inhibits Zp activation by Jun, then CK2β (but not CK2α) should inhibit EBV reactivation. To test this hypothesis, CK2α and CK2β were individually silenced with specific siRNA in AGS-EBV cells, followed by NaB/TPA treatment to induce reactivation, and effects on BZLF1 and BMRF1 lytic protein expression were examined (Fig. 6A). Silencing of CK2α had little effect on lytic protein expression. In contrast, CK2β silencing resulted in a notable increase in lytic protein expression. These experiments were repeated in HONE1 nasopharyngeal carcinoma cells containing latent Akata EBV (HONE1-Akata) (Fig. 6B). Again, silencing of CK2β but not CK2α led to a striking increase in EBV lytic proteins. These results confirm a role for CK2β in suppressing EBV reactivation that is independent of its role as part of the CK2 kinase, supporting the model that CK2β mediates the interaction between ARKL1 and Jun.

ARKL1 localizes to the BZLF1 promoter. The discovery of the ARKL1-Jun interaction and the inhibition of Jun activity by ARKL1 suggests that ARKL1 may suppress BZLF1 transcription by binding to promoter-associated Jun or, alternatively, could sequester Jun away from the promoter, as shown in the models in Fig. 7A. To determine if ARKL1 can be recovered at the BZLF1 promoter, we expressed HA-ARKL1 with the Zp-luc reporter plasmid and performed chromatin immunoprecipitations (ChIPs) using hemagglutinin (HA) antibody (or IgG control antibody), followed by qPCR for Zp.

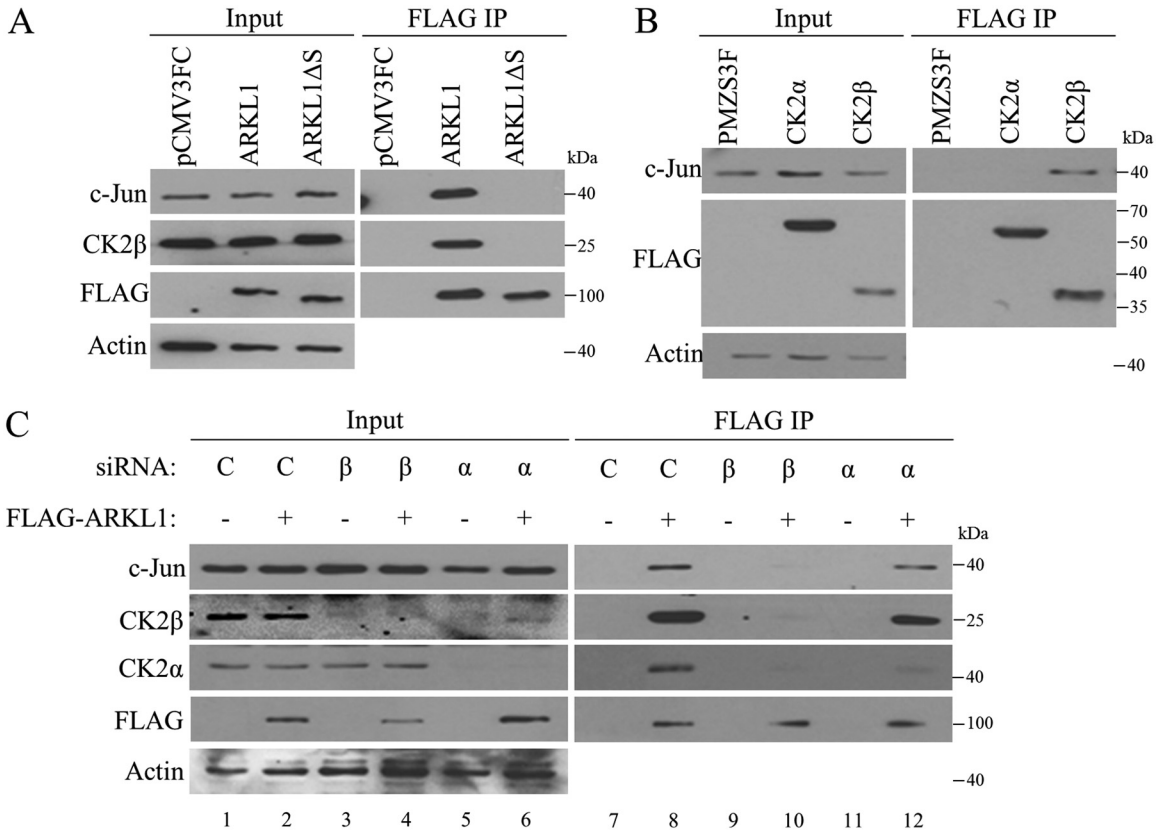

FIG 5 Requirements for ARKL1-Jun interaction. (A) AGS cells were transfected with FLAG-ARKL1, FLAG-ARKL1ΔS, or empty FLAG (pCMV3FC) expression plasmids followed by FLAG immunoprecipitation. Recovered proteins were analyzed by Western blotting using antibodies against c-Jun, CK2β, and FLAG. A total of 5% of input lysates are also shown along with actin loading control. (B) AGS cells were transfected with plasmids expressing FLAG-tagged CK2α, CK2β, or empty plasmid (pMZS3F), followed by FLAG-IPs and Western blotting as above using antibodies against c-Jun and FLAG. (C) AGS cells were treated with siRNA targeting CK2α (α) or CK2β (β) or negative-control (C) siRNA, followed by transfection of FLAG-ARKL1 (+) or empty expression plasmids (−). FLAG-IPs and Western blots were performed as described above using antibodies against Jun, FLAG, CK2α, and CK2β.

Recovery of Zp was found to be greatly increased by HA-ARKL1 compared with the empty vector control (Fig. 7B), supporting the model in which ARKL1 associates with Zp. The ChIP experiment with HA-ARKL1 was repeated comparing recovery of Zp-luc to a luciferase reporter plasmid lacking Zp, and the results confirmed the importance of Zp element (Fig. 7C). We also examined effects of overexpressing CK2β, Jun, or both on

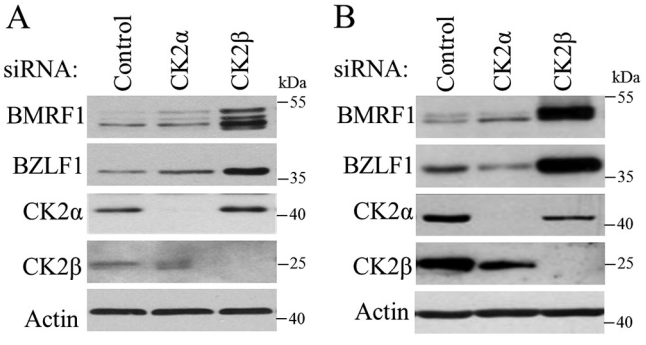

FIG 6 CK2β silencing promotes EBV reactivation. AGS-EBV (A) or HONE1-Akata (B) cells were transfected with siRNA targeting CK2α or CK2β or negative-control siRNA, followed by treatment with NaB/TPA. Equal amounts of lysates were then compared by Western blotting using antibodies against BMRF1, BZLF1, CK2α, CK2β, and actin.

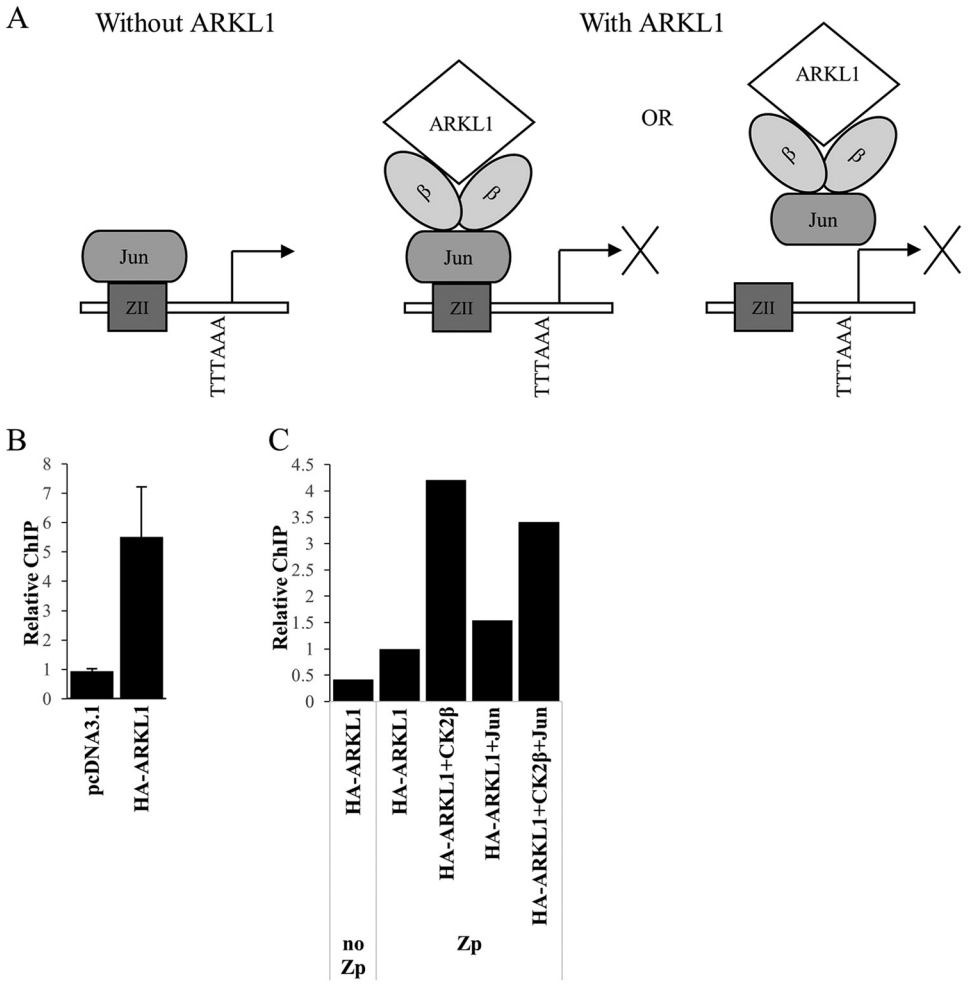

FIG 7 Model and ChIP of ARKL1 interaction with Zp. (A) Model of possible roles for ARKL1 in suppressing EBV reactivation. In the absence of ARKL1, Jun binds to the Zp to activate BZLF1 transcription promoting EBV reactivation. In the presence of ARKL1, ARKL1 can interact with Jun through CK2β to either negatively regulate Jun activity at the BZLF1 promoter or sequester Jun away from the Zp promoter. (B) ChIP of HA-ARKL1 on Zp. AGS cells were transfected with HA-ARKL1 expression plasmid or empty vector pcDNA3.1 along with Zp-luc reporter plasmid followed by formaldehyde cross-linking. ChIP was performed on sheared chromatin using HA or negative-control IgG antibodies, and Zp was quantified by qPCR. Fold enrichment of chromatin with HA antibody over IgG control was determined, and the recovery of Zp with HA-ARKL1 relative to empty plasmid pcDNA3.1 is displayed. Average values from two independent experiments is shown along with their standard deviations. (C) AGS cells were transfected with luciferase reporter plasmid with (Zp-luc; Zp) or without (pGL4.10-luc; no Zp) Zp, a second plasmid expressing HA-ARKL1, and, where indicated, additional plasmids expressing FLAG-CK2β and/or FLAG-c-Jun. ChIP assays were performed as in (B). Recovery of chromatin with HA antibody was normalized to IgG, and the Zp recovery from each sample is shown relative to the sample transfected with HA-ARKL1 and Zp only.

the ChIP results and found that both proteins could increase recovery of ARKL1 at Zp (Fig. 7C). This supports the model that ARKL1 associates with Zp through CK2β and Jun.

DISCUSSION

Life-long infection by EBV depends on its ability to alternate between latent and lytic infection cycles. Reactivation to the lytic state is important not only for the horizontal transmission of the virus but also for the increase in latent infection in some compartments due to increased viral load. As a result, high lytic infection predicts an increased risk of some EBV-associated cancers, including nasopharyngeal carcinoma (2, 56, 57). In addition, while EBV-induced cancers are considered to be latent infections, expression of subsets of lytic proteins is common and is thought to drive oncogenesis (58–61). However, the proteins and mechanisms that control EBV reactivation and specific lytic protein expression are not well understood. Here, we have identified

ARKL1 as a cellular protein that can inhibit EBV reactivation by suppressing expression of the EBV BZLF1 lytic switch protein that controls reactivation of EBV.

Reactivation to the EBV lytic cycle can occur in both B cells and epithelial cells, although the oral epithelium is the most prominent site of lytic infection (62–64). We examined the effect of ARKL1 on EBV infection in the context of gastric carcinoma (AGS) cells, NPC (NPC43) cells, and B cells and, in all cases, found that ARKL1 suppresses reactivation of EBV to the lytic cycle. Importantly, all of the EBV-positive cell lines we used had a low level of spontaneous reactivation, which allowed us to assess effects of ARKL1 modulation on reactivation in the absence of chemical treatments that are commonly used to reactivate EBV (such as TPA and sodium butyrate) but also have multiple effects on the cell. Subsequent experiments showed that ARKL1 acted on the promoter of the BZLF1 lytic switch protein (Zp), suggesting that repression of Zp and BZLF1 expression is at least part of the mechanism by which ARKL1 suppresses EBV reactivation.

A proteomic experiment identified Jun as an interactor of ARKL1. Jun was previously shown to be associated with Zp and to activate transcription of BZLF1 (23, 27, 29). Moreover, high levels of Jun are thought to be an important factor in the high degree of EBV reactivation in AGS cells (29). Since ARKL1 suppresses Zp, we tested the possibility that ARKL1 did so by inhibiting Jun activity. Consistent with this hypothesis, we showed that ARKL1 overexpression suppressed Jun activity in a Jun reporter assay. Some EBV lytic proteins in addition to BZLF1 can be directly regulated by AP-1 transcription factors, such as Jun (28, 65, 66). Therefore, the effect of ARKL1 on the EBV lytic cycle may not be limited to regulation of BZLF1 expression, although that alone would have a major impact on lytic infection.

We previously identified ARKL1 as a protein that interacted with CK2β through the KSSR binding pocket and showed that this interaction was mediated by a polyserine region of ARKL1 (44). Our ARKL1 proteomic experiment (Table 1) confirmed CK2β (and associated CK2α) as a prominent interaction. Additionally, we found that the ARKL1 polyserine region was required for the Jun interaction, suggesting that this interaction might be mediated by either CK2β or the CK2 holoenzyme. This possibility was further supported by the finding that depletion of CK2β disrupted the ARKL1-Jun interaction and led to induction of BZLF1 expression. Similar effects were not seen when CK2α was depleted, suggesting that CK2β was acting independently of CK2α in this regard. The model that CK2β mediates the ARKL1-Jun interaction (Fig. 7A) is further supported by coimmunoprecipitation of Jun with CK2β but not CK2α (Fig. 5B). Interestingly, Jun was previously reported to be negatively regulated by phosphorylation by CK2, indicating multiple roles of CK2 in regulating Jun activity (67). In addition, phosphorylation of BZLF1 by CK2 has been shown to regulate BZLF1's ability to repress expression of an EBV late gene (68). Our results suggest a novel role for CK2β that is independent of the CK2 holoenzyme. The possibility that CK2β can function independently of CK2α is also supported by previous reports that cellular CK2β levels are in excess of the CK2 catalytic subunits and that CK2β is detected in cellular locations devoid of the catalytic subunits (43, 69).

We have identified ARKL1 as a negative regulator of EBV reactivation, suggesting that high ARKL1 levels would promote latency and decrease lytic infection. Interestingly, a study by Domingues et al. (49) also identified ARKL1 as a factor inhibiting influenza A virus infection, although the mechanism of this effect was not determined. In addition, ARKL1 expression was shown to be repressed by human T-cell leukemia virus type I (HTLV-1) infection (70), suggesting that interference with ARKL1 is also beneficial to this virus. Overall, these results point to an antiviral function of ARKL1. While the cellular functions of ARKL1 have yet to be determined, our findings on the mechanism of ARKL1 repression of EBV reactivation indicate that ARKL1 can suppress Jun activity. This suggests that ARKL1 might also have a similar role in regulating Jun activation of cellular genes, including Jun target genes involved in proliferation, differentiation, and apoptosis (71–74).

ARKL1 was first identified as a SUMO-interacting protein (75, 76) and was also shown

to be highly modified by SUMO2 in response to influenza A virus infection (49). SUMOylation is central to antiviral responses, and conversely, manipulation of the SUMO pathway is a strategy employed by many viruses to regulate antiviral responses and promote infections (77–79). It is currently unclear how SUMOylation of ARKL1 (as observed in response to influenza virus infection) affects ARKL1 activity and whether SUMOylation of ARKL1 impacts EBV reactivation. However, SUMOylation in general promotes latency of EBV and other herpesviruses and must be overcome during reactivation (78, 80, 81), suggesting that SUMO modification of ARKL1 might be required to repress EBV reactivation. The mechanism by which ARKL1 represses Jun activity also remains to be determined. Since ARKL1 contains SUMO interacting motifs (SIMs) similar to those in Arkadia, it is possible that the ARKL1 SIMs may influence its protein-protein interactions as reported for Arkadia (47). SIMs in Arkadia have been shown to mediate an interaction with the CBX4 component of Polycomb repressive complex 1 (PRC1) involved in transcriptional repression of target genes (47). It will be interesting to determine if ARKL1 also associates with CBX4/PRC1 to exert its suppressive effect on Jun and EBV reactivation.

Reactivation of EBV is largely controlled by activation of BZLF1 expression, and several cellular proteins have been reported to activate or repress the BZLF1 promoter (10, 11). Here, we add to this complicated regulation by showing that the uncharacterized ARKL1 protein represses BZLF1 expression through effects on Jun, a known activator of Zp. Moreover, we define a role for CK2β in mediating this interaction and regulating EBV reactivation, providing a novel and unexpected function for this kinase subunit.

MATERIALS AND METHODS

Cell lines. AGS cells containing recombinant neomycin-resistant EBV (AGS-EBV) derived from Akata-Burkitt's lymphoma (82) were cultured in RPMI 1640 medium (Gibco) supplemented with 10% fetal bovine serum (FBS). NPC43 cells containing EBV from recurrent NPC tissues (51) were grown in RPMI media containing 10% FBS, and 4 μM Y-27632 (Enzo Life Sciences). B cells containing M81 EBV, provided by Henri-Jacques Delecluse (52), were maintained in RPMI medium containing 10% FBS. Human embryonic kidney 293T cells were cultured in Dulbecco modified Eagle medium (DMEM) with 10% FBS. HONE1-Akata cells, an NPC cell line infected with Akata EBV (83), were maintained in α-MEM (Gibco) supplemented with 10% FBS.

Plasmids. Triple FLAG-tagged ARKL1 was generated by inserting the coding sequence of ARKL1 in the multiple cloning site of the triple FLAG containing pCMV3FC plasmid between the BglII and NotI sites. The ARKL1ΔS mutant lacking amino acids 202 to 226 was generated by gene synthesis, described in Cao et al. (44), and inserted into the same restriction sites of the pCMV3FC plasmid as above. The plasmids expressing FLAG-DDX24, FLAG-FBXO38, and FLAG-BKRF4 are described previously (84–86). The BZLF1 promoter firefly luciferase (pZp-luc) and renilla luciferase plasmids (pRL-TK) were kindly provided by Takayuki Murata (53). FLAG-c-Jun and 5xTRE firefly luciferase plasmids are described in Vikhanskaya et al. (87) and provided by Kanuga Sabapathy. FLAG-CK2α and FLAG-CK2β were generated by insertion of the coding sequence of the respective genes from the pGEX-3X CK2α and CK2β plasmids (provided by David Litchfield) into the pMZS3F vector containing C-terminal calmodulin binding peptide and triple FLAG tags (SPA tag). CK2α was inserted between the XbaI and NotI sites using the forward primer 5′-GATCT CTAGAGGCCATGGAGGCCATGTCGGGACCCGTGCCAAG-3′ and reverse primer 5′-GGATCCGCGGCCGCACT GCTGAGCGCCAGC-3′. CK2β was inserted between the XhoI and NotI sites using the forward primer 5′-GATCGGCCATGGAGGCCCTCGAGATGAGCAGCTCAGAGGAGG-3′ and reverse primer 5′-GATCGGATCCC TAGCGGCCGCAGCGAATCGTCTTGACTGGG-3′. HA-ARKL1 was generated by inserting the coding sequence of ARKL1 between the HindIII and NotI sites of the pcDNA3.1 vector (placing triple HA-tags at the C terminus), using the forward primer 5′-GATCAAGCTTGCCACCATGAAGATGGAGGAGGCAGTGG-3′ and reverse primer 5′-GTGAGCGGCCGCGCCAGTAGGTATTTACGCCTGC-3′.

ARKL1 overexpression in AGS-EBV. AGS-EBV cells were plated in 6-well dishes containing poly-L-lysine-treated coverslips and transfected with 2 μg of plasmids expressing FLAG-ARKL1, FLAG-DDX24, FLAG-FBXO38, or FLAG-BKRF4, using 6 μl of linear polyethylenimine (PEI; catalog number 23966; Polyscience Inc.) according to the manufacturer's instructions. In some experiments, cells were treated with 3 mM sodium butyrate (NaB) and 20 ng/ml 12-*O*-tetradecanoylphorbol-13-acetate (TPA) 24 hours post-transfection to induce the lytic cycle. At 24 hours postinduction, cells were fixed with 3.7% formaldehyde for 20 minutes, permeabilized with 1% Triton X-100 for 5 minutes, and blocked with 4% bovine serum albumin (BSA) for 1 hour. Cells were stained with FLAG (1:1,000 dilution; catalog no. 740001; Invitrogen) and BZLF1 (1:100 dilution; catalog no. sc-53904; Santa Cruz) primary antibodies for 1 hour followed by 1:700 dilution of goat anti-rabbit Alexa Fluor 488 and goat anti-mouse Alexa Fluor 555 secondary antibodies for 1 hour. Coverslips were mounted onto slides using ProLong Gold antifade fluorescent mounting medium (Invitrogen) containing 4′,6-diamidino-2-phenylindole (DAPI). Images were obtained

using 40× oil objective on a Leica DMi8 inverted fluorescence microscope and analyzed using Leica LasX software. At least 100 transfected cells were counted for each experiment, in three biological replicates.

ARKL1 silencing experiments in AGS-EBV. AGS-EBV cells were plated in 6-cm dishes and transfected with 120 pmol of ARKL1-specific siRNA1 (5′-ACGCAGUAUGUUAGCACCAGGCAAA-3′), siRNA2 (5′-CAUCUGCUGGCAAUGCGCCACUCAA-3′) or AllStars negative-control siRNA (Qiagen) using 2 μl of Lipofectamine 2000 (Thermo Fisher Scientific). The cells were subjected to two additional rounds of silencing after 24 and 48 hours. In some experiments, 24 hours after the third round, cells were treated with 3 mM NaB and 20 ng/ml TPA to induce the lytic cycle and harvested 24 hours post-drug treatment for Western blot analysis. In all cases, cells were lysed in 9 M urea and 10 mM Tris (pH 6.8), followed by sonication. A total of 30 μg of drug-induced and 100 μg of uninduced lysates were subjected to 10% SDS-PAGE and transferred to nitrocellulose membrane. Membranes were blocked with 5% skim milk in phosphate-buffered saline with 0.1% Tween (PBS-T) for 1 hour, followed by overnight incubation with primary antibodies ARKL1 (1:200 dilution; catalog no. sc-86701; Santa Cruz), BMRF1 (1:2,000 dilution; catalog no. MAB8186; Millipore), BZLF1 (1:1,000 dilution; catalog no. sc-53904; Santa Cruz), and β-actin (1:10,000 dilution; catalog no. sc-47778; Santa Cruz) prepared in the blocking buffer. Membranes were washed with PBS-T and incubated with donkey anti-goat (1:5,000 dilution; catalog no. SAB3700285-1; Sigma) or goat anti-mouse (1:5,000 dilution; catalog no. sc-2005; Santa Cruz) secondary antibodies for 1 hour. Membranes were washed with PBS-T, and signals were detected by enhanced chemiluminescence (catalog no. sc-2048; Santa Cruz). Band quantifications were performed using ImageQuant software (GE Healthcare Life Sciences).

ARKL1 silencing in NPC43 cells and M81 B cells. Lentiviral plasmids (pLKO.1-puro) containing three different short hairpin RNAs (shRNAs) targeting ARKL1 (pLKO.1-shARKL1) as described in reference 49 were kindly supplied by Ben Hale and were used to generate lentivirus in 293T cells using standard methods. NPC43 cells or M81 B cells (1×10^5) were infected using Polybrene (Sigma) at a final concentration of 8 μg/ml with 500 μl of cultured medium containing shARKL1 or shControl lentivirus. At 24 hours postinfection, the medium was replaced with fresh growth medium containing 2 μg/ml puromycin, and cells were grown for at least 72 hours to select for cells with the integrated lentivirus. M81 cells were transduced with a second round of lentivirus 7 days after the first round. Harvested cells were lysed in 9 M urea and 10 mM Tris (pH 6.8), and 70 to 100 μg (NPC43 cells) or 50 μg (M81 cells) of clarified lysate was subjected to 10% SDS-PAGE and Western blotted as described above with ARKL1, BZLF1, and actin primary antibodies and donkey anti-goat or goat anti-mouse secondary antibodies. Band quantifications were performed as described above.

ARKL1 effect on BZLF1 mRNA transcripts. AGS-EBV were plated in 6-well dishes and either subjected to ARKL1 silencing or overexpression. Briefly, for ARKL1 silencing, AGS-EBV cells were transfected with 100 pmol of siRNA1 using Lipofectamine 2000 for 3 days and harvested 48 hours after the last round of siRNA transfection. For overexpression, AGS-EBV cells were transfected with 1 μg of plasmids expressing empty vector pCMV3FC or FLAG-ARKL1 using 3 μl PolyJet and harvested 48 hours posttransfection. Total RNA was extracted using NucleoZOL (Macherey-Nagel) according to the manufacturer's instructions. One microgram of total RNA was treated with 0.5 units of DNase I (New England BioLabs) for 15 min. One-step real-time quantitative PCR (RT-qPCR) was performed with 1/10 of the DNase I-treated mRNA using a Luna Universal one-step RT-qPCR kit (New England BioLabs) with a reaction volume of 10 μl in a CFX384 real-time system (Bio-Rad). Primers used for BZLF1 mRNA quantification were described previously (88). The relative mRNA expression level was derived from $2-\Delta\Delta CT$ by use of the comparative threshold cycle (C_T) method. The amount of mRNA in each sample was normalized to the amount of actin mRNA. Western blots were also performed with lysates from overexpression samples using antibodies against FLAG and vinculin (1:10,000 dilution; catalog no. sc-25336; Santa Cruz).

Reporter assays with ARKL1 overexpression. For pZp-luc assays, AGS cells were plated in 6-well dishes and then transfected with 0.9 μg plasmids expressing FLAG-ARKL1 or empty vector pCMV3FC, along with 10 ng of pZp-luc reporter and 30 ng of pRL-TK (renilla control) plasmids using 4 μl PolyJet transfection reagent (SignaGen Laboratories) as per manufacturer's instructions. For TRE-luc assays without Jun overexpression, AGS cells were transfected as above along with 10 ng of 5XTRE-luc and 30 ng pRL-TK. For TRE-luc assays with Jun overexpression, AGS cells were transfected with 0.9 μg plasmids expressing FLAG-ARKL1 or empty vector pCMV3FC in addition to 0.9 μg plasmid expressing c-Jun, along with 20 ng 5xTRE-luc and 60 ng pRL-TK. In both assays, cells were harvested 48 hours posttransfection, lysed in passive lysis buffer (PLB) (Promega), and clarified by centrifugation. Luciferase assays were performed using a dual-luciferase reporter assay system (Promega) and a GloMax 20/20 luminometer (Promega). Firefly luciferase reporter values were normalized to renilla luciferase values to control for transfection efficiency.

Zp reporter assay with ARKL1 silencing. AGS cells were plated in 6-well dishes and transfected with 100 pmol of ARKL1-specific siRNA1 using Lipofectamine 2000. This transfection was repeated 24 and 48 hours later. Five hours after the third transfection, cells were transfected with 10 ng pZp-luc, 30 ng pRL-TK, and 0.9 μg pCMV3FC empty plasmids using 4 μl PolyJet transfection reagent. Forty-eight hours later, cells were lysed in PLB and clarified by centrifugation. Luciferase activities were measured and normalized as described above.

Affinity purification-mass spectrometry (AP-MS). HEK293T cells in three 10-cm dishes were transfected with 5 μg of empty plasmid pCMV3FC or plasmid expressing FLAG-ARKL1 using 10 μl PolyJet transfection reagent. Cells were transferred to 15-cm dishes and lysed 48 hours posttransfection in modified radioimmunoprecipitation assay (RIPA) buffer (50 mM Tris-HCl [pH 8.0], 300 mM NaCl, 0.1% sodium deoxycholate, 0.5% NP-40, and 2 mM EDTA) with phosphatase (Halt; Sigma) and protease

inhibitor cocktail (catalog no. P8340; Sigma). FLAG-ARKL1 and associated proteins were recovered on M2 anti-FLAG resin (catalog no. A2220; Sigma-Aldrich) as described in Cao et al. (44). Recovered proteins were trypsinized and processed for tandem liquid chromatography-mass spectrometry (LC-MS/MS) as previously described (44) and analyzed using a linear trap quadropole (LTQ) orbitrap system (Thermo Finnigan) and Mascot software (Matrix Science, United Kingdom).

Immunoprecipitation of Jun with FLAG-ARKL1. AGS cells were plated in 10-cm dishes and transfected with 7 μg of plasmids expressing FLAG-ARKL1 WT, FLAG-ARKL1ΔS, or empty plasmid pCMV3FC using 21 μl PEI transfection reagent. Cells were harvested 48 hours posttransfection and lysed in modified RIPA buffer with sonication. Lysates were clarified by centrifugation, and then 1 mg lysate was incubated with 5 μl of M2 anti-FLAG resin for 3 hours at 4°C with mixing. Resin was collected by centrifugation, washed in modified RIPA buffer, and boiled in 2× SDS buffer. Immunoprecipitated proteins were subjected to SDS-PAGE and analyzed by Western blotting using primary antibodies against c-Jun (1:1,000 dilution; catalog no. 711202; ThermoFisher Scientific), FLAG (1:20,000 dilution; catalog no. 740001; Invitrogen), CK2β (1:1,000 dilution; catalog no. 2072-1; Epitomics), and β-actin (1:10,000 dilution; catalog no. sc-47778; Santa Cruz) as described above.

Immunoprecipitation of Jun with FLAG-ARKL1 upon CK2 silencing. AGS cells in 10-cm dishes were transfected with 250 pmol of siRNA targeting CK2α (5′-CCCAUAAUGUCAUGAUUGAUCAUGA-3′), CK2β (5′-UCGGAUGGAUCUUGAAACC[dT][dT]-3′), or AllStars negative-control siRNA (Qiagen) using 2 μl of Lipofectamine 2000, followed by two additional rounds of silencing after 24 and 48 hours. Seven hours later, cells were transfected with 7 μg of FLAG-ARKL1 or pCMV3FC empty vector using PEI. Forty-eight hours later, cells were harvested in modified RIPA buffer and sonicated. Lysates were clarified by centrifugation, and then 700 μg lysate was incubated with 8 μl of M2 anti-FLAG resin for 3 hours at 4°C with mixing. Resin was collected by centrifugation, washed in modified RIPA buffer, and boiled in 2× SDS buffer. Immunoprecipitated proteins were subjected to SDS-PAGE and analyzed by Western blotting using primary antibodies against c-Jun, FLAG, CK2α (1:5,000 dilution; catalog no. A300-198A; Bethyl), CK2β, and β-actin as described above.

CK2-Jun interaction IP. AGS cells in 10-cm dishes were transfected with 7 μg of pMZS3F-CK2α, pMZS3F-CK2β, or pMZS3F empty vector using PEI transfection reagents according to the manufacturer's protocol. Cells were harvested 48 hours posttransfection and lysed in modified RIPA buffer with sonication. IPs and Western blots were performed as described above.

CK2 silencing on EBV reactivation. AGS-EBV or HONE1-Akata cells were plated in 6-cm dishes and transfected with 100 pmol of siRNA against CK2α, CK2β, or AllStars negative-control siRNA using 1 μl of Lipofectamine 2000 as mentioned above. The cells were subjected to two additional rounds of silencing after 24 and 48 hours. Twenty-four hours later, cells were transferred to 10-cm dishes and induced for EBV reactivation with 3 mM NaB and 20 ng/ml TPA. Cells were harvested 24 hours postinduction and lysed in RIPA buffer (50 mM Tris-HCl [pH 8], 150 mM NaCl, 0.5% NP-40, 0.1% sodium deoxycholate, 2 mM EDTA, and 1 mM sodium fluoride and protease inhibitors cocktail) followed by sonication. A total of 25 μg of clarified lysates was subjected to 10% SDS-PAGE and Western blotting as described above with primary antibodies against BMRF1, BZLF1, CK2α, CK2β (1:500 dilution; catalog no. sc-20710; Santa Cruz), and actin and secondary antibodies goat anti-mouse, goat anti-rabbit, or donkey anti-goat.

HA-ARKL1 ChIP at Zp. AGS cells in two 10-cm dishes were transfected with 4 μg of empty plasmid pcDNA3.1 or plasmid expressing HA-ARKL1 along with 4 μg of Zp-luc using 24 μl PEI. Forty-eight hours posttransfection, cells were cross-linked with formaldehyde (1% final concentration) for 10 mins at room temperature. Chromatin immunoprecipitation (ChIP) assays of HA-ARKL1 on Zp were performed using the SimpleChIP enzymatic chromatin IP kit (catalog no. 9003; Cell Signaling Technologies). Fragmented chromatin was subjected to nuclease treatment for 20 minutes at 37°C before sonication. ChIP was performed on 5 μg of digested chromatin using 2 μg of HA (catalog no. sc-7392X; Santa Cruz) or normal mouse IgG (catalog no. sc-2343; Santa Cruz) antibodies overnight followed by recovery on protein G magnetic beads for 2 hours. Immunoprecipitated DNA was quantified by quantitative real-time PCR (qPCR) with the CFX384 real-time system (Bio-Rad) using the primers for Zp promoter (Zp0) described previously (17). Fold enrichment of chromatin recovered with HA antibody over IgG control within each sample condition was calculated. To determine the effect of overexpression of CK2β and c-Jun on ARKL1 recovery of Zp, AGS cells in two 10-cm dishes were transfected with 2 μg of ARKL1, 2 μg of Zp-luc, or empty luciferase vector pGL4.10-luc and 2 μg of FLAG-CK2β and/or FLAG-c-Jun for a total of 8 μg plasmids transfected (empty plasmid pcDNA3.1 was added to bring the total plasmid amount to 8 μg as needed) using 24 μl PEI. Cells were harvested 48 hours posttransfection and subjected to ChIP as detailed above. Chromatin recovered with HA antibody was normalized to IgG control.

Statistics. Statistical analysis was performed using the paired Student's *t* test using Microsoft Excel. Data represent averages from three independent experiments along with their standard deviations. Significance is indicated as follows: ns, no significance; *, $P \leq 0.05$; **, $P \leq 0.01$; ***, $P \leq 0.001$; and ****, $P \leq 0.0001$.

ACKNOWLEDGMENTS

We thank Jennifer Yinuo Cao for generating FLAG-CK2α and FLAG-CK2β expression plasmids, David Litchfield for pGEX-3X CK2α and CK2β plasmids, and Kanuga Sabapathy and Takayuki Murata for luciferase reporter plasmids. We also thank Ben Hale for ARKL1 shRNA constructs and Henri-Jacques Delecluse for M81 B cells.

This work was supported by Canadian Institutes of Health Research project grant

153014 (to L.F.) and Research Grant Council, Hong Kong (grants C7027-16G and GRF-106180141) to S.W.T.

REFERENCES

1. Gershburg E, Pagano JS. 2005. Epstein-Barr virus infections: prospects for treatment. J Antimicrob Chemother 56:277–281. https://doi.org/10.1093/jac/dki240.
2. Young LS, Yap LF, Murray PG. 2016. Epstein-Barr virus: more than 50 years old and still providing surprises. Nat Rev Cancer 16:789–802. https://doi.org/10.1038/nrc.2016.92.
3. Elgui de Oliveira D, Müller-Coan BG, Pagano JS. 2016. Viral carcinogenesis beyond malignant transformation: EBV in the progression of human cancers. Trends Microbiol 24:649–664. https://doi.org/10.1016/j.tim.2016.03.008.
4. Chen JN, He D, Tang F, Shao CK. 2012. Epstein-Barr virus-associated gastric carcinoma: a newly defined entity. J Clin Gastroenterol 46:262–271. https://doi.org/10.1097/MCG.0b013e318249c4b8.
5. Lee JH, Kim Y, Choi JW, Kim YS. 2014. Prevalence and prognostic significance of Epstein-Barr virus infection in classical Hodgkin's lymphoma: a meta-analysis. Arch Med Res 45:417–431. https://doi.org/10.1016/j.arcmed.2014.06.001.
6. Murata T, Sato Y, Kimura H. 2014. Modes of infection and oncogenesis by the Epstein-Barr virus. Rev Med Virol 24:242–253. https://doi.org/10.1002/rmv.1786.
7. Kempkes B, Robertson ES. 2015. Epstein-Barr virus latency: current and future perspectives. Curr Opin Virol 14:138–144. https://doi.org/10.1016/j.coviro.2015.09.007.
8. Hammerschmidt W, Sugden B. 2013. Replication of Epstein-Barr viral DNA. Cold Spring Harb Perspect Biol 5:a013029. https://doi.org/10.1101/cshperspect.a013029.
9. Mckenzie J, El-Guindy A. 2015. Epstein-Barr virus lytic cycle reactivation. Curr Top Microbiol Immunol 391:237–261. https://doi.org/10.1007/978-3-319-22834-1_8.
10. Murata T. 2014. Regulation of Epstein-Barr virus reactivation from latency. Microbiol Immunol 58:307–317. https://doi.org/10.1111/1348-0421.12155.
11. Kenney SC, Mertz JE. 2014. Regulation of the latent-lytic switch in Epstein-Barr virus. Semin Cancer Biol 26:60–68. https://doi.org/10.1016/j.semcancer.2014.01.002.
12. Speck SH, Chatila T, Flemington E. 1997. Reactivation of Epstein-Barr virus: regulation and function of the BZLF1 gene. Trends Microbiol 5:399–405. https://doi.org/10.1016/S0966-842X(97)01129-3.
13. Farrell PJ, Rowe DT, Rooney CM, Kouzarides T. 1989. Epstein-Barr virus BZLF1 trans-activator specifically binds to a consensus AP-1 site and is related to c-fos. EMBO J 8:127–132. https://doi.org/10.1002/j.1460-2075.1989.tb03356.x.
14. Heston L, El-Guindy A, Countryman J, Dela Cruz C, Delecluse H-J, Miller G. 2006. Amino acids in the basic domain of Epstein-Barr virus ZEBRA protein play distinct roles in DNA binding, activation of early lytic gene expression, and promotion of viral DNA replication. J Virol 80:9115–9133. https://doi.org/10.1128/JVI.00909-06.
15. Lieberman PM. 2015. Chromatin structure of Epstein-Barr virus latent episomes. Curr Top Microbiol Immunol 390:71–102. https://doi.org/10.1007/978-3-319-22822-8_5.
16. Hammerschmidt W. 2015. The epigenetic life cycle of Epstein-Barr virus. Curr Top Microbiol Immunol 390:103–117. https://doi.org/10.1007/978-3-319-22822-8_6.
17. Murata T, Kondo Y, Sugimoto A, Kawashima D, Saito S, Isomura H, Kanda T, Tsurumi T. 2012. Epigenetic histone modification of Epstein-Barr virus BZLF1 promoter during latency and reactivation in Raji cells. J Virol 86:4752–4761. https://doi.org/10.1128/JVI.06768-11.
18. Baumann M, Mischak H, Dammeier S, Kolch W, Gires O, Pich D, Zeidler R, Delecluse HJ, Hammerschmidt W. 1998. Activation of the Epstein-Barr virus transcription factor BZLF1 by 12-*O*-tetradecanoylphorbol-13-acetate-induced phosphorylation. J Virol 72:8105–8114.
19. Hausen HZ, O'Neill FJ, Freese UK, Hecker E. 1978. Persisting oncogenic herpesvirus induced by the tumour promoter TPA. Nature 272:373–375. https://doi.org/10.1038/272373a0.
20. Falk KI, Ernberg I. 1999. Demethylation of the Epstein-Barr virus origin of lytic replication and of the immediate early gene BZLF1 is DNA replication independent. Arch Virol 144:2219–2227. https://doi.org/10.1007/s007050050636.
21. Faggioni A, Zompetta C, Grimaldi S, Barile G, Frati L, Lazdins J. 1986. Calcium modulation activates Epstein-Barr virus genome in latently infected cells. Science 232:1554–1556. https://doi.org/10.1126/science.3012779.
22. Daibata M, Speck SH, Mulder C, Sairenji T. 1994. Regulation of the BZLF1 promoter of Epstein-Barr virus by second messengers in anti-immunoglobulin-treated B cells. Virology 198:446–454. https://doi.org/10.1006/viro.1994.1056.
23. Flemington E, Speck SH. 1990. Identification of phorbol ester response elements in the promoter of Epstein-Barr virus putative lytic switch gene BZLF1. J Virol 64:1217–1226.
24. Borras AM, Strominger JL, Speck SH. 1996. Characterization of the ZI domains in the Epstein-Barr virus BZLF1 gene promoter: role in phorbol ester induction. J Virol 70:3894–3901.
25. Liu S, Borras AM, Liu P, Suske G, Speck SH. 1997. Binding of the ubiquitous cellular transcription factors Sp1 and Sp3 to the ZI domains in the Epstein-Barr virus lytic switch BZLF1 gene promoter. Virology 228:11–18. https://doi.org/10.1006/viro.1996.8371.
26. Murata T, Narita Y, Sugimoto A, Kawashima D, Kanda T, Tsurumi T. 2013. Contribution of myocyte enhancer factor 2 family transcription factors to BZLF1 expression in Epstein-Barr virus reactivation from latency. J Virol 87:10148–10162. https://doi.org/10.1128/JVI.01002-13.
27. Wang YCJ, Huang JM, Montalvo EA. 1997. Characterization of proteins binding to the ZII element in the Epstein-Barr virus BZLF1 promoter: transactivation by ATF1. Virology 227:323–330. https://doi.org/10.1006/viro.1996.8326.
28. Yu K-P, Heston L, Park R, Ding Z, Wang'ondu R, Delecluse H-J, Miller G. 2013. Latency of Epstein-Barr virus is disrupted by gain-of-function mutant cellular AP-1 proteins that preferentially bind methylated DNA. Proc Natl Acad Sci U S A 110:8176–8181. https://doi.org/10.1073/pnas.1301577110.
29. Feng W, Kraus RJ, Dickerson SJ, Lim HJ, Jones RJ, Yu X, Mertz JE, Kenney SC. 2007. ZEB1 and c-Jun levels contribute to the establishment of highly lytic Epstein-Barr virus infection in gastric AGS cells. J Virol 81:10113–10122. https://doi.org/10.1128/JVI.00692-07.
30. Flemington E, Speck SH. 1990. Autoregulation of Epstein-Barr virus putative lytic switch gene BZLF1. J Virol 64:1227–1232.
31. Mansouri S, Wang S, Frappier L. 2013. A role for the nucleosome assembly proteins TAF-Iβ and NAP1 in the activation of BZLF1 expression and Epstein-Barr virus reactivation. PLoS One 8:e63802. https://doi.org/10.1371/journal.pone.0063802.
32. Bhende PM, Dickerson SJ, Sun X, Feng W-H, Kenney SC. 2007. X-box-binding protein 1 activates lytic Epstein-Barr virus gene expression in combination with protein kinase D. J Virol 81:7363–7370. https://doi.org/10.1128/JVI.00154-07.
33. Kraus RJ, Perrigoue JG, Mertz JE. 2003. ZEB negatively regulates the lytic-switch BZLF1 gene promoter of Epstein-Barr virus. J Virol 77:199–207. https://doi.org/10.1128/jvi.77.1.199-207.2003.
34. Ellis AL, Wang Z, Yu X, Mertz JE. 2010. Either ZEB1 or ZEB2/SIP1 can play a central role in regulating the Epstein-Barr virus latent-lytic switch in a cell-type-specific manner. J Virol 84:6139–6152. https://doi.org/10.1128/JVI.02706-09.
35. Yu X, Wang Z, Mertz JE. 2007. ZEB1 regulates the latent-lytic switch in infection by Epstein-Barr virus. PLoS Pathog 3:1993–2004. https://doi.org/10.1371/journal.ppat.0030194.
36. Liu P, Liu S, Speck SH. 1998. Identification of a negative *cis* element within the ZII domain of the Epstein-Barr virus lytic switch BZLF1 gene promoter. J Virol 72:8230–8239.
37. Yu X, McCarthy PJ, Lim H-J, Iempridee T, Kraus RJ, Gorlen DA, Mertz JE. 2011. The ZIIR element of the Epstein-Barr virus BZLF1 promoter plays a central role in establishment and maintenance of viral latency. J Virol 85:5081–5090. https://doi.org/10.1128/JVI.02615-10.
38. Frappier L. 2015. EBNA1. Curr Top Microbiol Immunol 391:3–34. https://doi.org/10.1007/978-3-319-22834-1_1.
39. Frappier L. 2012. Contributions of Epstein-Barr nuclear antigen 1 (EBNA1) to

cell immortalization and survival. Viruses 4:1537–1547. https://doi.org/10.3390/v4091537.
40. Sivachandran N, Sarkari F, Frappier L. 2008. Epstein-Barr nuclear antigen 1 contributes to nasopharyngeal carcinoma through disruption of PML nuclear bodies. PLoS Pathog 4:e1000170. https://doi.org/10.1371/journal.ppat.1000170.
41. Malik-Soni N, Frappier L. 2012. Proteomic profiling of EBNA1-host protein interactions in latent and lytic Epstein-Barr virus infections. J Virol 86:6999–7002. https://doi.org/10.1128/JVI.00194-12.
42. Sivachandran N, Cao JY, Frappier L. 2010. Epstein-Barr virus nuclear antigen 1 hijacks the host kinase CK2 to disrupt PML nuclear bodies. J Virol 84:11113–11123. https://doi.org/10.1128/JVI.01183-10.
43. Litchfield DW. 2003. Protein kinase CK2: structure, regulation and role in cellular decisions of life and death. Biochem J 369:1–15. https://doi.org/10.1042/BJ20021469.
44. Cao JY, Shire K, Landry C, Gish GD, Pawson T, Frappier L. 2014. Identification of a novel protein interaction motif in the regulatory subunit of casein kinase 2. Mol Cell Biol 34:246–258. https://doi.org/10.1128/MCB.00968-13.
45. Pickard BS, Malloy MP, Clark L, Lehellard S, Ewald HL, Mors O, Porteous DJ, Blackwood DHR, Muir WJ. 2005. Candidate psychiatric illness genes identified in patients with pericentric inversions of chromosome 18. Psychiatr Genet 15:37–44. https://doi.org/10.1097/00041444-200503000-00007.
46. Erker Y, Neyret-Kahn H, Seeler JS, Dejean A, Atfi A, Levy L. 2013. Arkadia, a novel SUMO-targeted ubiquitin ligase involved in PML degradation. Mol Cell Biol 33:2163–2177. https://doi.org/10.1128/MCB.01019-12.
47. Sun H, Liu Y, Hunter T. 2014. Multiple Arkadia/RNF111 structures coordinate its Polycomb body association and transcriptional control. Mol Cell Biol 34:2981–2995. https://doi.org/10.1128/MCB.00036-14.
48. Poulsen SL, Hansen RK, Wagner SA, van Cuijk L, van Belle GJ, Streicher W, Wikström M, Choudhary C, Houtsmuller AB, Marteijn JA, Bekker-Jensen S, Mailand N. 2013. RNF111/Arkadia is a SUMO-targeted ubiquitin ligase that facilitates the DNA damage response. J Cell Biol 201:797–807. https://doi.org/10.1083/jcb.201212075.
49. Domingues P, Golebiowski F, Tatham MH, Lopes AM, Taggart A, Hay RT, Hale BG. 2015. Global reprogramming of host SUMOylation during influenza virus infection. Cell Rep 13:1467–1480. https://doi.org/10.1016/j.celrep.2015.10.001.
50. Mansouri S, Pan Q, Blencowe BJ, Claycomb JM, Frappier L. 2014. Epstein-Barr virus EBNA1 protein regulates viral latency through effects on let-7 MicroRNA and dicer. J Virol 88:11166–11177. https://doi.org/10.1128/JVI.01785-14.
51. Lin W, Yip YL, Jia L, Deng W, Zheng H, Dai W, Ko JMY, Lo KW, Chung GTY, Yip KY, Lee S-D, Kwan J-H, Zhang J, Liu T, Chan J-W, Kwong D-W, Lee V-F, Nicholls JM, Busson P, Liu X, Chiang AKS, Hui KF, Kwok H, Cheung ST, Cheung YC, Chan CK, Li B, Cheung A-M, Hau PM, Zhou Y, Tsang CM, Middeldorp J, Chen H, Lung ML, Tsao SW. 2018. Establishment and characterization of new tumor xenografts and cancer cell lines from EBV-positive nasopharyngeal carcinoma. Nat Commun 9:4663. https://doi.org/10.1038/s41467-018-06889-5.
52. Tsai MH, Raykova A, Klinke O, Bernhardt K, Gärtner K, Leung CS, Geletneky K, Sertel S, Münz C, Feederle R, Delecluse HJ. 2013. Spontaneous lytic replication and epitheliotropism define an Epstein-Barr virus strain found in carcinomas. Cell Rep 5:458–470. https://doi.org/10.1016/j.celrep.2013.09.012.
53. Murata T, Sato Y, Nakayama S, Kudoh A, Iwahori S, Isomura H, Tajima M, Hishiki T, Ohshima T, Hijikata M, Shimotohno K, Tsurumi T. 2009. TORC2, a coactivator of cAMP-response element-binding protein, promotes Epstein-Barr virus reactivation from latency through interaction with viral BZLF1 protein. J Biol Chem 284:8033–8041. https://doi.org/10.1074/jbc.M808466200.
54. Mellacheruvu D, Wright Z, Couzens AL, Lambert JP, St-Denis NA, Li T, Miteva YV, Hauri S, Sardiu ME, Low TY, Halim VA, Bagshaw RD, Hubner NC, Al-Hakim A, Bouchard A, Faubert D, Fermin D, Dunham WH, Goudreault M, Lin ZY, Badillo BG, Pawson T, Durocher D, Coulombe B, Aebersold R, Superti-Furga G, Colinge J, Heck AJR, Choi H, Gstaiger M, Mohammed S, Cristea IM, Bennett KL, Washburn MP, Raught B, Ewing RM, Gingras AC, Nesvizhskii AI. 2013. The CRAPome: a contaminant repository for affinity purification-mass spectrometry data. Nat Methods 10:730–736. https://doi.org/10.1038/nmeth.2557.
55. Liang CL, Chen JL, Hsu YPP, Ou JT, Chang YS. 2002. Epstein-Barr virus BZLF1 gene is activated by transforming growth factor-β through cooperativity of smads and c-Jun/c-Fos proteins. J Biol Chem 277:23345–23357. https://doi.org/10.1074/jbc.M107420200.
56. Cao SM, Liu Z, Jia WH, Huang QH, Liu Q, Guo X, Huang TB, Ye W, Hong MH. 2011. Fluctuations of Epstein-Barr virus serological antibodies and risk for nasopharyngeal carcinoma: a prospective screening study with a 20-year follow-up. PLoS One 6:e19100. https://doi.org/10.1371/journal.pone.0019100.
57. Ji MF, Wang DK, Yu YL, Guo YQ, Liang JS, Cheng WM, Zong YS, Chan KH, Ng SP, Wei WI, Chua DTT, Sham JST, Ng MH. 2007. Sustained elevation of Epstein-Barr virus antibody levels preceding clinical onset of nasopharyngeal carcinoma. Br J Cancer 96:623–630. https://doi.org/10.1038/sj.bjc.6603609.
58. Borozan I, Zapatka M, Frappier L, Ferretti V. 2018. Analysis of Epstein-Barr virus genomes and expression profiles in gastric adenocarcinoma. J Virol 92:e01239-17. https://doi.org/10.1128/JVI.01239-17.
59. Martel-Renoir D, Grunewald V, Touitou R, Schwaab G, Joab I. 1995. Qualitative analysis of the expression of Epstein-Barr virus lytic genes in nasopharyngeal carcinoma biopsies. J Gen Virol 76:1401–1408. https://doi.org/10.1099/0022-1317-76-6-1401.
60. Lin Z, Xu G, Deng N, Taylor C, Zhu D, Flemington EK. 2010. Quantitative and qualitative RNA-seq-based evaluation of Epstein-Barr virus transcription in type I latency Burkitt's lymphoma cells. J Virol 84:13053–13058. https://doi.org/10.1128/JVI.01521-10.
61. Hu L, Lin Z, Wu Y, Dong J, Zhao B, Cheng Y, Huang P, Xu L, Xia T, Xiong D, Wang H, Li M, Guo L, Kieff E, Zeng Y, Zhong Q, Zeng M. 2016. Comprehensive profiling of EBV gene expression in nasopharyngeal carcinoma through paired-end transcriptome sequencing. Front Med 10:61–75. https://doi.org/10.1007/s11684-016-0436-0.
62. Tsao SW, Tsang CM, To KF, Lo KW. 2015. The role of Epstein-Barr virus in epithelial malignancies. J Pathol 235:323–333. https://doi.org/10.1002/path.4448.
63. Hutt-Fletcher LM. 2014. Epstein-Barr virus replicating in epithelial cells. Proc Natl Acad Sci U S A 111:16242–16243. https://doi.org/10.1073/pnas.1418974111.
64. Temple RM, Zhu J, Budgeon L, Christensen ND, Meyers C, Sample CE. 2014. Efficient replication of Epstein-Barr virus in stratified epithelium *in vitro*. Proc Natl Acad Sci U S A 111:16544–16549. https://doi.org/10.1073/pnas.1400818111.
65. Lyons DE, Yu KP, Heiden JA, Vander Heston L, Dittmer DP, El-Guindy A, Miller G. 2018. Mutant cellular AP-1 proteins promote expression of a subset of Epstein-Barr virus late genes in the absence of lytic viral DNA replication. J Virol 92:e01062-18. https://doi.org/10.1128/JVI.01062-18.
66. Packham G, Economou A, Rooney CM, Rowe DT, Farrell PJ. 1990. Structure and function of the Epstein-Barr virus BZLF1 protein. J Virol 64:2110–2116.
67. Lin A, Frost J, Deng T, Smeal T, Al-Alawi N, Kikkawa U, Hunter T, Brenner D, Karin M. 1992. Casein kinase II is a negative regulator of c-Jun DNA binding and AP-1 activity. Cell 70:777–789. https://doi.org/10.1016/0092-8674(92)90311-y.
68. El-Guindy AS, Miller G. 2004. Phosphorylation of Epstein-Barr virus ZEBRA protein at its casein kinase 2 sites mediates its ability to repress activation of a viral lytic cycle late gene by Rta. J Virol 78:7634–7344. https://doi.org/10.1128/JVI.78.14.7634-7644.2004.
69. Bibby AC, Litchfield DW. 2005. The multiple personalities of the regulatory subunit of protein kinase CK2: CK2 dependent and CK2 independent roles reveal a secret identity for CK2beta. Int J Biol Sci 1:67–79. https://doi.org/10.7150/ijbs.1.67.
70. Vernin C, Thenoz M, Pinatel C, Gessain A, Gout O, Delfau-Larue MH, Nazaret N, Legras-Lachuer C, Wattel E, Mortreux F. 2014. HTLV-1 bZIP factor HBZ promotes cell proliferation and genetic instability by activating oncomiRs. Cancer Res 74:6082–6093. https://doi.org/10.1158/0008-5472.CAN-13-3564.
71. Eferl R, Wagner EF. 2003. AP-1: a double-edged sword in tumorigenesis. Nat Rev Cancer 3:859–868. https://doi.org/10.1038/nrc1209.
72. Shaulian E, Karin M. 2002. AP-1 as a regulator of cell life and death. Nat Cell Biol 4:E131–E136. https://doi.org/10.1038/ncb0502-e131.
73. Hess J, Angel P, Schorpp-Kistner M. 2004. AP-1 subunits: quarrel and harmony among siblings. J Cell Sci 117:5965–5973. https://doi.org/10.1242/jcs.01589.
74. Gustems M, Woellmer A, Rothbauer U, Eck SH, Wieland T, Lutter D, Hammerschmidt W. 2014. C-Jun/c-Fos heterodimers regulate cellular genes via a newly identified class of methylated DNA sequence motifs. Nucleic Acids Res 42:3059–3072. https://doi.org/10.1093/nar/gkt1323.
75. Rosendorff A, Sakakibara S, Lu S, Kieff E, Xuan Y, DiBacco A, Shi Y, Shi Y,

Gill G. 2006. NXP-2 association with SUMO-2 depends on lysines required for transcriptional repression. Proc Natl Acad Sci U S A 103:5308–5313. https://doi.org/10.1073/pnas.0601066103.
76. Hecker C-M, Rabiller M, Haglund K, Bayer P, Dikic I. 2006. Specification of SUMO1- and SUMO2-interacting motifs. J Biol Chem 281:16117–16127. https://doi.org/10.1074/jbc.M512757200.
77. Lowrey AJ, Cramblet W, Bentz GL. 2017. Viral manipulation of the cellular sumoylation machinery. Cell Commun Signal 15:27. https://doi.org/10.1186/s12964-017-0183-0.
78. Wilson VG. 2017. Viral interplay with the host sumoylation system. Adv Exp Med Biol 963:359–388. https://doi.org/10.1007/978-3-319-50044-7_21.
79. Everett RD, Boutell C, Hale BG. 2013. Interplay between viruses and host sumoylation pathways. Nat Rev Microbiol 11:400–411. https://doi.org/10.1038/nrmicro3015.
80. Bentz GL, Moss CR, Whitehurst CB, Moody CA, Pagano JS. 2015. LMP1-induced sumoylation influences the maintenance of Epstein-Barr virus latency through KAP1. J Virol 89:7465–7477. https://doi.org/10.1128/JVI.00711-15.
81. Poole EL, Kew VG, Lau JCH, Murray MJ, Stamminger T, Sinclair JH, Reeves MB. 2018. A virally encoded deSUMOylase activity is required for cytomegalovirus reactivation from latency. Cell Rep 24:594–606. https://doi.org/10.1016/j.celrep.2018.06.048.
82. Borza CM, Hutt-Fletcher LM. 2002. Alternate replication in B cells and epithelial cells switches tropism of Epstein-Barr virus. Nat Med 8:594–599. https://doi.org/10.1038/nm0602-594.
83. Glaser R, Zhang HY, Yao KT, Zhu HC, Wang FX, Li GY, Wen DS, Li YP. 1989. Two epithelial tumor cell lines (HNE-1 and HONE-1) latently infected with Epstein-Barr virus that were derived from nasopharyngeal carcinomas. Proc Natl Acad Sci U S A 86:9524–9528. https://doi.org/10.1073/pnas.86.23.9524.
84. Yamauchi T, Nishiyama M, Moroishi T, Yumimoto K, Nakayama KI. 2014. MDM2 mediates nonproteolytic polyubiquitylation of the DEAD-box RNA helicase DDX24. Mol Cell Biol 34:3321–3340. https://doi.org/10.1128/MCB.00320-14.
85. Georges A, Coyaud E, Marcon E, Greenblatt J, Raught B, Frappier L. 2019. USP7 regulates cytokinesis through FBXO38 and KIF20B. Sci Rep 9:2724. https://doi.org/10.1038/s41598-019-39368-y.
86. Ho T-H, Sitz J, Shen Q, Leblanc-Lacroix A, Campos EI, Borozan I, Marcon E, Greenblatt J, Fradet-Turcotte A, Jin D-Y, Frappier L. 2018. A screen for Epstein-Barr virus proteins that inhibit the DNA damage response reveals a novel histone binding protein. J Virol 92:e00262-18. https://doi.org/10.1128/JVI.00262-18.
87. Vikhanskaya F, Toh WH, Dulloo I, Wu Q, Boominathan L, Ng HH, Vousden KH, Sabapathy K. 2007. p73 supports cellular growth through c-Jun-dependent AP-1 transactivation. Nat Cell Biol 9:698–706. https://doi.org/10.1038/ncb1598.
88. Wen W, Iwakiri D, Yamamoto K, Maruo S, Kanda T, Takada K. 2007. Epstein-Barr virus BZLF1 gene, a switch from latency to lytic infection, is expressed as an immediate-early gene after primary infection of B lymphocytes. J Virol 81:1037–1042. https://doi.org/10.1128/JVI.01416-06.